Applied Clay Science 269 (2025) 107758

Contents lists available at ScienceDirect

Applied Clay Science

journal homepage: www.elsevier.com/locate/clay

Research Paper

Modified natural mineral with a biogenic compound to control microbial growth in waterborne paint

Leyanet Barberia-Roque [a], Guillermo P. Lopez [a,b], Erasmo Gámez-Espinosa [a,b], Katerine Igal [a], Mariela A. Fernández [b,c], Cecilia Deyá [a,b], Natalia Bellotti [a,b,*]

[a] CIDEPINT-Centro de Investigación y Desarrollo en Tecnología de Pinturas y Recubrimientos (CICPBA-CONICET-UNLP)- Calle 52 e/ 121 y 122, La Plata, Buenos Aires, Argentina
[b] UNLP-Universidad Nacional de La Plata, Buenos Aires, Argentina
[c] CETMIC- Centro de Tecnología de Recursos Minerales y Cerámica (CONICET-CICPBA)-Camino Centenario y 506, M.B. Gonnet, Buenos Aires, Argentina

ARTICLE INFO

Keywords:
Montmorillonite
Essential oil
Hybrid
Hygienic paint
Biocide
Biodeterioration

ABSTRACT

Hygienic paints are designed to control microbial growth by imparting antimicrobial activity both in-film and in-can. Biogenic compounds like terpenes in essential oils (EOs) have potential antimicrobial properties. Additionally, modified montmorillonites (Mt) show promise as nanoscale carriers for these compounds. This research aimed to obtain a functionalized antimicrobial montmorillonite hybrid to be applied in the formulation of bioactive paints. The biogenic compounds evaluated were the essential oils of white thyme and mint, to be applied for the first time in hygienic coatings. A soybean derivative was used as an organic modifier of the clay mineral. The synthesized hybrids were characterized by Fourier-Transform Infrared (FTIR) spectroscopy, X-ray diffraction (XRD), thermogravimetric analysis (TGA), scanning electron microscopy (SEM), and energy dispersive spectrometer (EDS). Bioassays were carried out against fungal strains including *Cladosporium cladosporioides*, *Chaetomium globosum*, and *Aspergillus versicolor*, as well as bacterial strains such as *Staphylococcus aureus* and *Escherichia coli*. White thyme was the EO with the higher antimicrobial activity. Added to this, white thyme oil managed to impart its antimicrobial activity to the synthesized hybrid. The formulated paints with 0.75 concentration of pigment per volume (PVC) efficiently prevented in-can pollution.

1. Introduction

The proliferation of microorganisms in building materials poses significant economic, environmental, and health challenges. Microbial growth accelerates material degradation, leading to increased maintenance costs and compromised structural integrity (Cámara et al., 2022; Romani et al., 2022). Additionally, the proliferation of microorganisms compromised indoor air quality, affecting the health of occupants and increasing the risk of respiratory diseases (Felgueiras et al., 2022; Sánchez Espinosa et al., 2024). Waterborne paints, particularly those using acrylic resin and water as a solvent, are highly susceptible to microbial degradation due to carbon sources in the formulation that support microbial growth both in storage and after application (Kakakhel et al., 2019; Mardones et al., 2019). While bacteria dominate in aqueous environments like paint containers, fungi are the primary agents of in-film deterioration (Gillatt et al., 2015). Calcium carbonate deposition by environmental bacteria further exacerbates paint degradation, as it is a key component in many latex paints (Chen et al., 2022a; Chen et al., 2022b). These issues highlight the urgent need for effective antimicrobial strategies to preserve materials, protect public health, and reduce environmental impacts (Gámez-Espinosa et al., 2020b). Recent advancements in antimicrobial coatings focus on integrating bioactive and environmentally friendly biocides, such as biogenic compounds and nanomaterials, to enhance functionality and safety (Bellotti and Deyá, 2020; Qiu et al., 2024). Nanomaterials, including bioinspired antimicrobial peptides and capsaicin-derived polymers, have shown promise in medical applications (Majhi et al., 2019; Freitas et al., 2022; Zhou et al., 2023). Similarly, plant extracts and EOs from *Eucalyptus globulus*, *Melaleuca cajuputi*, rosemary, cinnamon, and guarana exhibit notable antimicrobial activity in film and coating formulations (Bonilla and Sobral, 2016; Andrade et al., 2018; Farina Farizan et al., 2024; Majeed et al., 2024).

* Corresponding author at: CIDEPINT-Centro de Investigación y Desarrollo en Tecnología de Pinturas y Recubrimientos (CICPBA-CONICET-UNLP)- Calle 52 e/ 121 y 122, La Plata, Buenos Aires, Argentina.
E-mail address: n.bellotti@cidepint.ing.unlp.edu.ar (N. Bellotti).

https://doi.org/10.1016/j.clay.2025.107758
Received 1 October 2024; Received in revised form 5 February 2025; Accepted 15 February 2025
Available online 18 February 2025

EOs contain terpenes, many of which are even approved for use in the food industry by the Food and Drug Administration (FDA), and generally recognized as safe (GRAS) for specific uses (Chen and Viljoen, 2022; Zhuang et al., 2023; U.S. Food and Drug Administration-FDA, 2024). Terpenes are a diverse group synthesized through the isoprenoid pathway and are classified based on the number of isoprene units in their structure. For example, monoterpenes (C_{10}) are made from two isoprene units, sesquiterpenes (C_{15}) from three, and diterpenes (C_{20}) from four isoprene units (Câmara et al., 2024). These compounds are known for their distinctive aromatic qualities and various biological activities, including antimicrobial, anti-inflammatory, and antioxidant properties (Mamusa et al., 2021; Mangalagiri et al., 2021). Some terpenes, such as thymol, carvacrol, and eugenol, are particularly noted for their antibacterial effects and are often found in essential oils used in medicinal applications (Raut and Karuppayil, 2014; Guimarães et al., 2019).

However, the volatility of EOs and their terpene components limits their effectiveness in long-term applications, necessitating strategies like encapsulation or incorporation into solid supports such as clays to enhance stability and sustained release (Liu et al., 2021; Fattahi et al., 2023). Various strategies are being explored to efficiently integrate these compounds into formulations through encapsulation or incorporating them into natural solid supports, such as clays, which are cost-effective and highly suitable for coating formulations (Gonçalves et al., 2017; Ryu et al., 2018; Fernández et al., 2020).

Clays such as montmorillonite (Mt), kaolinite (Kaol), and bentonite (Bent) possess extensive surface areas and porous structures, offering numerous active sites for adsorption (Nagy et al., 2013; Hendessi et al., 2016; Hossain et al., 2023). These properties enable clays to act as stable matrices for controlled release systems, protecting bioactive compounds from degradation and ensuring prolonged antimicrobial efficacy (de Oliveira et al., 2022). This approach has been shown to improve the stability and effectiveness of bioactive agents in coatings, as highlighted in studies on clay-based nanocomposites used in various antimicrobial applications (Fernández et al., 2020; Mamusa et al., 2021; García-Guzmán et al., 2023).

This study focuses on developing bioactive clay hybrids with biogenic compounds for antimicrobial paint formulation. The biogenic compounds tested were EOs of: white thyme (EW) and mint (EM), extracted from *Thymus masticina* L. and *Mentha* sp. L., respectively. Thyme EO is rich in thymol and carvacrol (terpenes) which are the main antimicrobial agents and are commonly found in EOs from other plants (Walentowska and Foksowicz-Flaczyk, 2013; Gonçalves et al., 2017). *Mentha* spp. are well-known for their medicinal properties (anti-inflammatory, anti-emetic, antispasmodic, analgesic, antidiabetic, etc.), with reports suggesting some antimicrobial and antioxidant effects of their EOs (Eftekhari et al., 2021). In a previous study, clay was modified with a terpene compound, citronellol, to be applied in antimicrobial coatings (Fernández et al., 2020). The present work expands on this concept by utilizing a mixture of terpene compounds, as the EOs, instead of a single, pure biogenic compound. As a novelty, this approach leverages chemical diversity to broaden the potential for antimicrobial activity.

Mt. sourced from Río Negro, Argentina, was employed in this study. This clay is abundant and cost-effective, offering a promising material for various applications, including catalysis, adsorption, and environmental remediation (Barraqué et al., 2018; Ciğeroğlu et al., 2024). Moreover, Mt. has been extensively studied as an adsorbent and has proven effective in removing heavy metals and organic compounds (Mendonça et al., 2019; Capelezzo et al., 2023). Its layered structure, large internal surface area, and high cation exchange capacity render it a promising material for applications such as functional antimicrobial material (de Oliveira et al., 2022; Wang et al., 2023).

EW and EM were evaluated as potential antimicrobials for waterborne paints. Soy lecithin (SLe) a natural and low-cost surfactant, served as an organic modifier for Mt. (Nagy et al., 2013; Fernández et al., 2020). SLe is positively charged at acid pH due to its amino groups; this allows the Mt. modification through the exchange with the corresponding Na^+ ions, which allows obtaining the hybrid with hydrophobic characteristics that can integrate biogenic compounds such as essential oils and terpenoids (Nagy et al., 2013).

The bioactivity of EO, Mt. hybrids, and coatings was assessed through conventional agar plate assays. Fungal strains, *Aspergillus versicolor* (MG725821), *Cladosporium cladosporioides* (MG731215), and *Chaetomium globosum* (KU936228), were isolated from biodeteriorated walls in previous research (Gámez-Espinosa et al., 2020a). Bacterial strains, *Escherichia coli* (ATCC 11229) and *Staphylococcus aureus* (ATCC 6538), were selected for their ubiquity and potential as pathogens (Weber et al., 2016). The synthesized Mt. hybrids were characterized using Fourier transform infrared spectroscopy (FTIR), X-ray diffraction (XRD), thermogravimetric analysis (TGA), and zeta potential (*ZP*).

2. Materials and methods

2.1. Materials

High-purity Na-montmorillonite (>99 %) used in this study was sourced from the Lago Pellegrini deposit in Río Negro, Argentina, and provided by Castiglioni Pes and Cia with the following composition: SiO_2 51.10 wt%, Al_2O_3 19.25 wt%, Fe_2O_3 4.83w%, Na_2O 2.31 wt%, CaO 1.39 %, MgO 1.32 %, TiO_2 0.24 wt%, K_2O 0.18 wt% (Magnoli et al., 2008). The purification method performed was based on fractionation by sedimentation to remove the majority of impurities (Bergaya and Lagaly, 2013). Its main properties were cation exchange capacity (*CEC*) = 82.5 mmol (100 g)$^{-1}$ determined by the *Cu*-triethylenetetramine method (Czímerová et al., 2006); specific surface area (*SSA*) was 34.0 m^2g^{-1} obtained by N_2 adsorption applying the BET equation, which represents the external specific surface area (Gamba et al., 2015).

Granular food-grade soybean lecithin (SLe) was obtained from Melar S.A., Buenos Aires, Argentina. The essential oils of white thyme (EW) and mint (EM) were supplied by Alfredo Francioni S.A., Buenos Aires, Argentina.

2.2. Antimicrobial activity of the biogenic compounds

To assess the antimicrobial activity of the commercial EOs (EW and EM) a screening of the antimicrobial potentialities was carried out by macrodilution method to determine the minimum inhibitory concentration (MIC) within the range of evaluated concentrations (Stupar et al., 2014; Fernández et al., 2020). For the fungal strains *C. globosum*, *A. versicolor,* and *C. cladosporioides*, 20 μL of a 10^5 spores/mL suspension was inoculated at the center of each malt extract agar (MEA) plate and incubated for 12 days at 28 °C. Radial growth was recorded by measuring the corresponding diameters. For the bacterial strains *E. coli* and *S. aureus*, the decrease in the number of colony-forming units (CFUs) was evaluated on Luria Bertani (LB) agar with different concentrations of the oils under study at 30 °C for 24 h, starting from a 10^6 CFU/mL culture. The same procedure was carried out with controls without any biocides. The assays were performed in triplicate. The most active EO was selected to be used in the hybrid clay synthesis.

2.3. Obtaining bioactive Mt. hybrids

The modified Mt. hybrid was obtained following a reported procedure by Fernandez et al. (Fernández et al., 2020). SLe, a positively charged organic surfactant at pH ≈ 2, was used to modify Mt. through ion exchange. This modification enhances its hydrophobicity, facilitating the integration of EO (Nagy et al., 2013). An ethanolic dissolution of SLe was prepared, and pH was adjusted to 2.3 by adding HCl 0.1 M. SLe was commercially obtained with food quality. The bioactive EO was mixed with the SLe dissolution in a 20 and 40 % wt concentration. The mix was incorporated into a recipient with the Mt. (pre-swollen) under

constant stirring, the ratio was 1:0.33 (Mt:SLe). Finally, Mt. hybrids were separated by centrifugation, dried and labeled as MtEW2 (Mt/EW/SLe 20 % wt) and MtEW4 (Mt/EW/SLe 40 % wt). The system composition to prepare the hybrids can be seen in Table 1.

2.4. Characterization

The FTIR spectra were obtained by using a Perkin Elmer (Spectrum ONE) FTIR spectrometer in the 4000–500 cm^{-1} spectral range. The analysis was performed directly on the sample using ATR (Attenuated Total Reflectance) with the U-ATR (Universal ATR Accessory) from PerkinElmer. The analysis was carried out with 16 scans, and the detector used was a TGS detector.

X-ray diffraction (XRD) was performed to obtain crystallographic data of the samples with a Philips 3710 diffractometer using Cu Kα radiation 40 kV, 40 mA, Ni filter and patterns collected from 3 to 12° (2θ). Diffractograms were obtained in the 2θ range of 3–70° with a step size of 0.02° and a step time of 0.5 s. Un-oriented samples were scanned and maintained at a constant relative humidity of 0.47 for 48 h to improve the precision of the peak values (Barraqué et al., 2018).

Thermogravimetric (TGA) analysis was carried out using a Rigaku Thermo plus EVO instrument, with alumina as reference. The temperature was increased at a constant rate of 10 °C/min. Pt crucibles were used to hold the samples and maintain at air atmosphere throughout the heating period, with a temperature range from 0 to 1000 °C. The temperature of each loss weight on the TGA was determined thorough the derivative TGA curve as a function of temperature (DTGA).

Zeta potential (*ZP*) was determined using the Brookhaven equipment (Zeta Potential function), at a constant ionic strength of 10^{-3} M KCl. Samples were prepared at different pH and equilibrated for 24 h by dropwise addition of HCl or KOH solutions. Electrophoretic mobility was converted into zeta potential values using the Smoluchowski equation (Fernández et al., 2020). For each determination, 40 mg of sample were dispersed in 40 mL of a 10^{-3} M KCl solution, the slurry was stirred, and pH was measured, and its value was labeled as natural pH.

Observations by scanning electron microscopy (SEM) to assess morphological aspects of the samples were carried out using Philips FEI SEM Quanta 200 under high vacuum conditions. The SEM was coupled to an EDS detector to analyze the elemental composition of the sample surfaces.

The antimicrobial activity was assessed by the agar diffusion well assay adapted from the Clinical and Laboratory Standards Institute (CLSI) method (CLSI et al., 2019; Fernández et al., 2020). Petri dishes were prepared by introducing 15 mL of culture medium (MEA for fungi and LB for bacteria) and inoculating them with 10^5 spores/mL and 10^6 CFU/mL suspensions, respectively. Subsequently, 7 mm diameter (D) wells were performed, and they were filled with 20 mg of the tested hybrid solids. Three replicates were performed for each case. All the plates were incubated at 28 °C for fungal strains and 30 °C for bacterial strains. After 24 and 48 h, respectively, the diameters of the inhibition zones were measured. In this regard, samples with $D < 7$ mm were inactive, while those with $D > 7$ mm were considered active. In the case of fungal strains, partial activity was considered, when $D = 7$ mm due to their characteristic invasive growth.

Table 1
Designation and amounts (wt%) of Mt., LSe, and EO (EW) used to prepare Mt./EO/SLe hybrids.

Sample	Mt (g)	LSe (g)	EO (g)
Mt-SLe	10	3.3	–
MtEW2	10	3.3	2
MtEW4	10	3.3	4

2.5. Formulation, preparation and characterization of paints

Paints were formulated with different concentrations of pigment per volume (PVCs) at 0.65, 0.75, and 0.85, as shown in Table 2. Control paints were prepared without biocide and labeled, CP6, CP7, and CP8. Mt. was incorporated at 5 % by weight, replacing an equivalent amount of talc in the paint formulations. The paints containing the clay hybrid (Mt/EO/SLe) were prepared using the same formulations, each with the same %wt of Mt. These were labeled, PW6, PW7, and PW8, corresponding to the different PVCs. The paint elaboration was carried out in the pilot plant of CIDEPINT using a high-speed disperser (Gámez-Espinosa et al., 2022).

The viscosity was determined at a controlled temperature of 25 ± 1 °C following the guidelines established by the IRAM 1109 A13 standard (April 2017 version). For this purpose, a 500 mL container was used, filled up to 0.2 cm from the edge with a digital Stormer Krebs Viscometer. The vane-type rotor measures 9 cm, in length and ends with two blades, each 2.7 cm long.

Water vapor transmission was assessed following ASTM D 1653, where the paints were applied to filter paper with a dry film thickness of 149 μm (calculated by measuring the difference in thickness between the uncoated and coated paper using a Schwyz coating thickness gauge). Non-corroding containers with silica gel, used as perm cups, were placed in a 100 % humidity chamber for 144 h. The weight change was measured using a scale, with the exposed area being 24 cm^2. The water vapor transmission was tracked by weighing the panels over a period of 336 h. The experimental data reported represents the average of three measurements for each sample. As a control, a paper filter without paint was also tested. Water vapor transmission is crucial because the paint's high permeability to water can negatively impact adhesion by disrupting the bonds between the substrate and the resin.

2.6. Bacterial resistance liquid paint test

The prepared paints (CP6, CP7, CP8, PW6, PW7, and PW8) together with a commercial paint (SW) and control paint (PVC = 0,8) without biocides and any clay (CP) were assessed for the bio-resistance to the bacterial growth in-can. The procedure followed was based on the ASTM D2574 standard. The strain used was *Pseudomona aeruginosa* (culture collection of the Department of Biological Sciences of the UNLP) which is recommended by the standard. *P. aeruginosa* culture incubated for 18 h at 30 °C in tryptic soy broth (TSB) medium was used to obtain the inoculum (OD = 0.1 at 600 nm). The assay was performed in sterile 24-well flat-bottom culture plates. In each well, 300 μL of inoculum in 3 g of paint were introduced, to achieve 10^6 CFU/g of final concentration. Triplicates were made for each sample. After the incubation period of 7 days, streaks in Petri plates with TSA were made for each well. All plates were incubated for 36 h at 30 °C. After this time, the plates were evaluated, and photographic registers were taken. The ASTM D2574 standard was used to rate the performance of the samples: 0 (no bacterial recovery); 1 (trace of contamination 1–9 colonies); 2 (light

Table 2
Paint composition (% by weight).

Compounds	CP6	CP7	CP8
Water	36.56	39.35	41.68
Q 202 (Antifoaming)	0.20	0.20	0.22
Mt	5.02	5.01	5.02
Polyacril D40 (Dispersant)	0.20	0.21	0.22
AMP-95 (Co-dispersant, neutralizing amine)	0.06	0.07	0.06
Triton 80 (Surfactant)	0.10	0.10	0.11
Sodium hexametaphosphate (Antisedimentant)	0.10	0.10	0.11
Talc	24.60	26.46	28.00
TiO_2	14.56	15.67	16.60
Resin (Thyosil, 1:1)	17.15	11.25	6.31
White spirit (Coalescent)	0.97	1.04	1.11
Butyl glycol (coalescent)	0.49	0.52	0.55

contamination, 10–99 colonies); 3 (moderate contamination, higher than 100 colonies) and 4 (heavy contamination, colonies indistinguishable) (ASTM D2574-16, 2020).

2.7. Fungal resistance coating test

The paints were applied on slide glasses and cured for 15 days under normal laboratory conditions and the same procedure reported in previous published research was followed (Bellotti et al., 2015). Three coating samples were disposed to each plate with minimum mineral medium and each one was inoculated with 50 μL of spore suspension (10^5 spores/mL). Six samples for each paint (CP6, CP7, CP8, PW6, PW7 and PW8) were assessed. The plates were incubated during a month at 28 °C. The same strains were used: *A. versicolor, C. cladosporioides* and *C. globosum*.

Biofilm growth was rated using the reference scale proposed by ASTM D5590 standard specification. The area covered by the fungal growth was referred to percentages (%): none, 0 %, trace, <10 %, light, 10–30 %, moderate, 30–60 %, and heavy, 60–100 % corresponding to a scale between 0 and 4, respectively (ASTM, 2001).

At the end of the bio-resistance test, coatings were observed by stereoscopic microscope, Leica S8 APO, and photographic records were taken by Leica MC 170 HD digital camera.

3. Results and discussion

3.1. Antimicrobial activity of the biogenic compounds

Fungal and bacterial inhibitory activity of the EW and EM were assessed, and the MIC was determined. The determined MIC values are presented in Table 3. Total fungal inhibition (100 %) was achieved with 0.3 and 0.6 mg/mL in the case of EW while concentrations equal to or greater than 1.2 mg/mL of EM were necessary to achieve complete inhibition. *S. aureus* was the most sensitive bacteria with a MIC of 0.15 mg/mL for both essential oils, while *E. coli* exhibited higher resistance, requiring a higher concentration of 1.2 mg/mL for complete inhibition for part of EW. Therefore, considering these results EW was the higher active EO and was chosen for the modified Mt.

The determined MICs for the studied EW, ranging from 0.15 to 1.2 mg/mL, demonstrate significant antimicrobial potential. This is consistent with findings from other studies involving similar fungal strains and the same plant species. Investigations into *Thymus leptobotrys* have highlighted its potent antifungal properties, with both its EO and chloroformic extract showing complete inhibition of fungi such as *Penicillium digitatum*, *Penicillium italicum*, and *Geotrichum candidum* (Lagrouh et al., 2017). Notably, the chloroformic extract achieved 100 % fungal growth inhibition at a concentration of 3 mg/mL, while the essential oil exhibited a maximum fungistatic effect at 1.2 mg/mL (Ameziane et al., 2007). These results were obtained through in vitro antifungal activity.

On the other hand, considering bibliographic information on commercial biocides, a comparison can be established with the natural products studied. For instance, Benzalkonium chloride and Preventol R80, which are widely utilized as antimicrobial agents, have reported MIC values in the range of 1.56 to 6.25 μL/mL against fungal strains as indicated in bibliographic data (Marco et al., 2020). This suggests that the studied compounds demonstrate comparable efficacy in microbial inhibition.

Furthermore, commonly used biocides to control in-film biodeterioration such as Carbendazim, 3-iodo-2-propynylbutylcarbamate (IPBC), and 2-n-octyl-4-isothiazolin-3-one (OIT), exhibited MIC values against comparable fungal strains, such as *Cladosporium cladosporioides*, *Chaetomium globosum*, and *Aspergillus niger* in the range of 0.5 to 10 μg/mL (equivalent to 0.0005–0.1 mg/mL) (Adan and Samson, 2011). Therefore, the MIC values of the studied compounds were approximately one order of magnitude higher than those reported in the literature for these commercial biocides.

Additionally, isothiazolinones, frequently employed for in-can preservation of waterborne paints, also serve as a benchmark for comparison. For example, 5-chloro-2-methyl-4-isothiazolin-3-one (CMIT) and 2-methyl-4-isothiazolin-3-one (MIT) require concentrations between 0.1 and 1 mg/mL to eliminate viable *Pseudomonas aeruginosa* cells, particularly those isolated from biofilms in paint tank environments (do Daulisio and Schneider, 2020). The MIC values of EO studied fall well within this range, highlighting their potential as effective antimicrobial agents for comparable applications. Unlike isothiazolinones and other commercial biocides, which are associated with significant ecotoxicological concerns, including harm to aquatic environments, cross-reactivity, and allergenic potential, biogenic compounds are not associated for now with decomposition into toxic byproducts under environmental conditions although this requires more research (Ferraz et al., 2022; Romani et al., 2022).

Table 3
Minimum inhibitory concentration (mg/mL) of EO against microbial strains.

	White thyme	Mint
A. versicolor	0.6	> 1.2
C. cladosporaides	≤ 0.3	> 1.2
C. globosum	0.3	1.2
E. coli	1.2	> 1.2
S. aureous	0.15	0.15

3.2. Characterization of Mt. hybrids

FTIR of Mt., Mt-SLe, MtEW2 (Mt/SLe/EW2) and MtEW4 (Mt/SLe/EW4) spectra are presented in Fig. 1. The modified Mt-SL, MtEW2 and MtEW4 presented new peaks such as 2928 cm^{-1}, 2855 cm^{-1}, 1730 cm^{-1}, 1470 cm^{-1} compared with the Mt. which correspond with C—H, C═O, and N—H groups (Chen et al., 2019). These functional groups founded in soybean lecithin remain after EW was added to the system. The modified Mt. hybrids and Mt. presented a peak 1630 cm^{-1} due to O—H stretching corresponding to the structural groups presented in the mineral (Nagy et al., 2013). The broadband region at 3400 cm^{-1}, which corresponds to O—H groups, was observed in all samples. Mt. exhibited peaks at 1039 and 914 cm^{-1}, corresponding to the stretching vibrations of Si—O and Al-O-Al, respectively (Giannakas et al., 2017; Xiao et al., 2024). The peak at 3639 $cm^{-1}$was attributed to the asymmetric stretching vibrations of OH bonded to Al and Si in Mt. (Xiao et al., 2024). In the case of modified Mt., the peak shifted to lower wavenumbers,

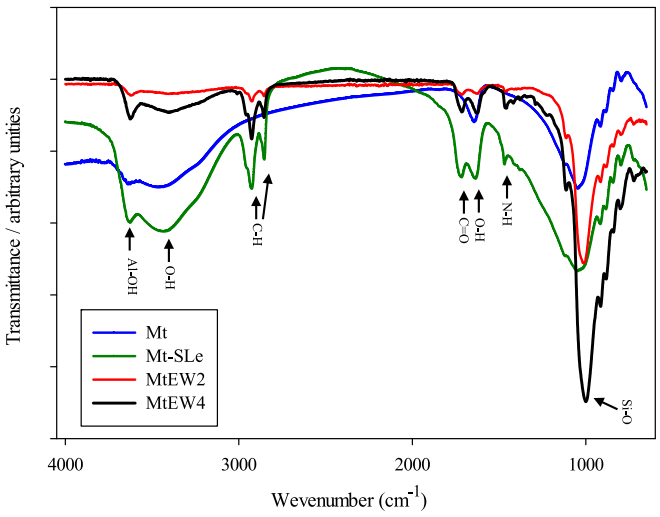

Fig. 1. FTIR spectra: Mt, Mt-SLe, MtEW2 and MtEW4.

specifically from 3639 to 3627 and 3628 cm^{-1} in Mt., Mt-SLe, and MtEW4, respectively. This shift would be induced by the migration of ions from the interlayer due to ionic exchange (He et al., 2020). The characteristic peaks corresponding with O—H and C—H were more intense in MtEW4 than in MtEW2 which could be related to a higher amount of EW retained in the mineral. The observed shift of the Si—O stretching bands to lower wavenumbers (from 1039 to 1009 cm^{-1}) in the hybrids could be due to chemical interactions or bonding between the Mt. framework and the modifying agents (SLe/EW). These interactions, which may involve hydrogen bonding or electrostatic forces (de Oliveira et al., 2022), would reduce the bond strength of Si—O as the modifiers introduce additional forces within the lattice structure (Madejová, 2003). A weaker bond vibrates at a lower frequency, leading to the observed downward shift in the FTIR spectrum. Additionally, some studies have associated the dehydration of Mt. with a downward shift of the Si—O stretching band (Lindholm et al., 2019). In this context, organic compound incorporation increased the hydrophobicity of the material, which promoted the expulsion of water molecules from the interlayer.

X-ray diffractograms of Mt., Mt-SL, MtEW2, and MtEW4 samples are presented in Fig. 2. Mt. sample exhibited a reflection peak d (001) plane at 1.26 nm (7° 2θ), indicating the structural predominance of a single-layer hydrate in the interlayer space. (Lagaly et al., 2006). The incorporation of the organic compounds expanded the interlayer space in 0.13 nm (to 1.39 nm) for the Mt-SLe sample. Considering that the basal spacing of dehydrated Mt. was reported as 0.97 nm the interlayer space thicknesses of Mt-SLe must be 0.42 nm which pointed out a bilayer arrangement of the SLe molecules (Barraqué et al., 2018). The basal spacing depends on the packing density of the surfactant within the Mt. interlayer space (He et al., 2006). The incorporation of EW further expanded the interlayer space by 0.18 nm (to 1.44 nm) and, as it was observed in the FTIR spectra, this corroborates the incorporation of the EW into the mineral structure. Considering previous research that evaluated the incorporation of one terpene, they obtained a higher expansion of the interlayer, ranging between 0.35 and 0.50 nm (Nagy et al., 2013; Fernández et al., 2020). This difference could be attributed to a more efficient arrangement of the antimicrobial agent when only a single type of terpenoid was used, as opposed to a mixture like EO.

The TGA analysis in Fig. 3 shows the weight loss % related to the modified Mt. (Mt-SLe, MtEW2, and MtEW4) and Mt. at different temperatures. The weight loss values are presented in Table 4. The TGA curves of Mt. and Mt-SLe indicate a mass loss between 20 and 100 °C of 13.1 % and 2.4 %, respectively. This mass loss was attributed to the evaporation of water adsorbed on the surface and within the interlayer space (Fernández Solarte et al., 2019). At temperatures above this range, the mass loss observed in Mt. corresponded to residual surface-adsorbed water and the dehydration of hydroxyl groups. In contrast, the greater mass loss in Mt-SLe at 100–700 °C was associated with the

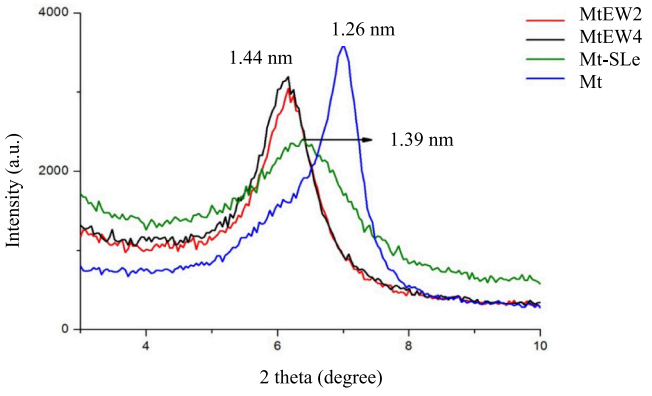

Fig. 2. XRD patterns: Mt., Mt-SLe, MtEW2 and MtEW4.

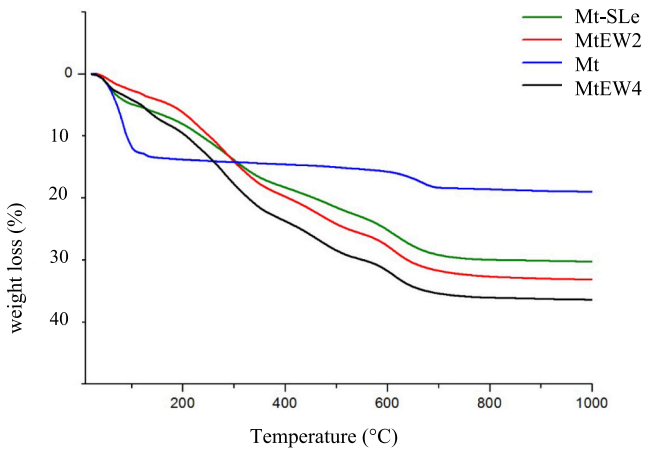

Fig. 3. TGA analysis: Mt., Mt-SLe, MtEW2 and MtEW4.

Table 4
Weight loss values of Mt. and hybrids determined from TGA curves.

Sample	Weight loss (%) at different temperature range (°C)		
	20–100	100–700	700–1000
Mt	13.1	6.9	2
Mt-SLe	2.4	19.9	≤2
MtEW2	2.9	24.9	≤2
MtEW4	3.8	28.8	≤2

decomposition of organic compounds (Fernández et al., 2020). The integration of the organic mix (EW/SLe) increased the mass loss of MtEW2 and MtEW4 in both temperature ranges (20–100 °C and 100–700 °C) compared to Mt-SLe from 19.9 to 24.9 and 28.8, respectively. This confirmed the successful incorporation of EW. This comparison gives us an idea of the amount of actual EO incorporated into the clay hybrid.

The *ZP* analysis (pH = 6.5) revealed that the external surface charge was modified by adding the SLe and EO, as indicated by the values determined to Mt-SLe (−26.04 mV), MtEW2 (−17.14 mV) and MtEW4 (−27.17 mV), which tend to be less negative compared to the Mt. (−34.24 mV) used to the synthesis. The loading of SLe and EW increased the surface charge of Mt. related to the cations exchange. The adsorbate interacts with the adsorbent surface by hydrogen bonds and electrostatic/hydrophobic interactions. The hydrophobic interaction may appear between the terpenes in the EO and the hydrophobic lecithin molecules adsorbed in the clay (Nakhli et al., 2018). The increase in EW concentration from 20 % to 40 % in the mix (EW/SLe) used in the synthesis while maintaining the Mt.:SLe ratio, likely enhanced the degree of terpene incorporation but potentially hindered Mt. surface interaction with the surfactant and led to less positive values for MtEW4 relative to MtEW2.

SEM micrographs and EDS analysis from Mt. and MtEW4 can be seen in Fig. 4a-d. Both samples showed micrometer-sized particles. MtWt4 presented greater agglomeration than the Mt. which could be corroborated in Fig. 4a and b. EDS spectra and semiquantitative analysis in Fig. 4c and d revealed the presence of the elements: O, Si, Al, C, Fe, Na, and Mg, each with a concentration exceeding 1 % by weight. The presence of O, Si, Al, Fe, Mg, and Na corroborates the chemical structure of the clay. The C detected on Mt. was attributed to the carbon tape used for sample mounting. The increase in the wt% of C element in MtWt4 sample (Fig. 4d) in comparison to Mt. (Fig. 4c) from 6.9 % to 36.0 % was attributed to the organic compounds incorporation (EW/SLe) by the functionalization.

The antimicrobial activity of the samples (MtEW2 and MtEW4) was assessed by the agar well diffusion test, in Table 5 the diameters of the

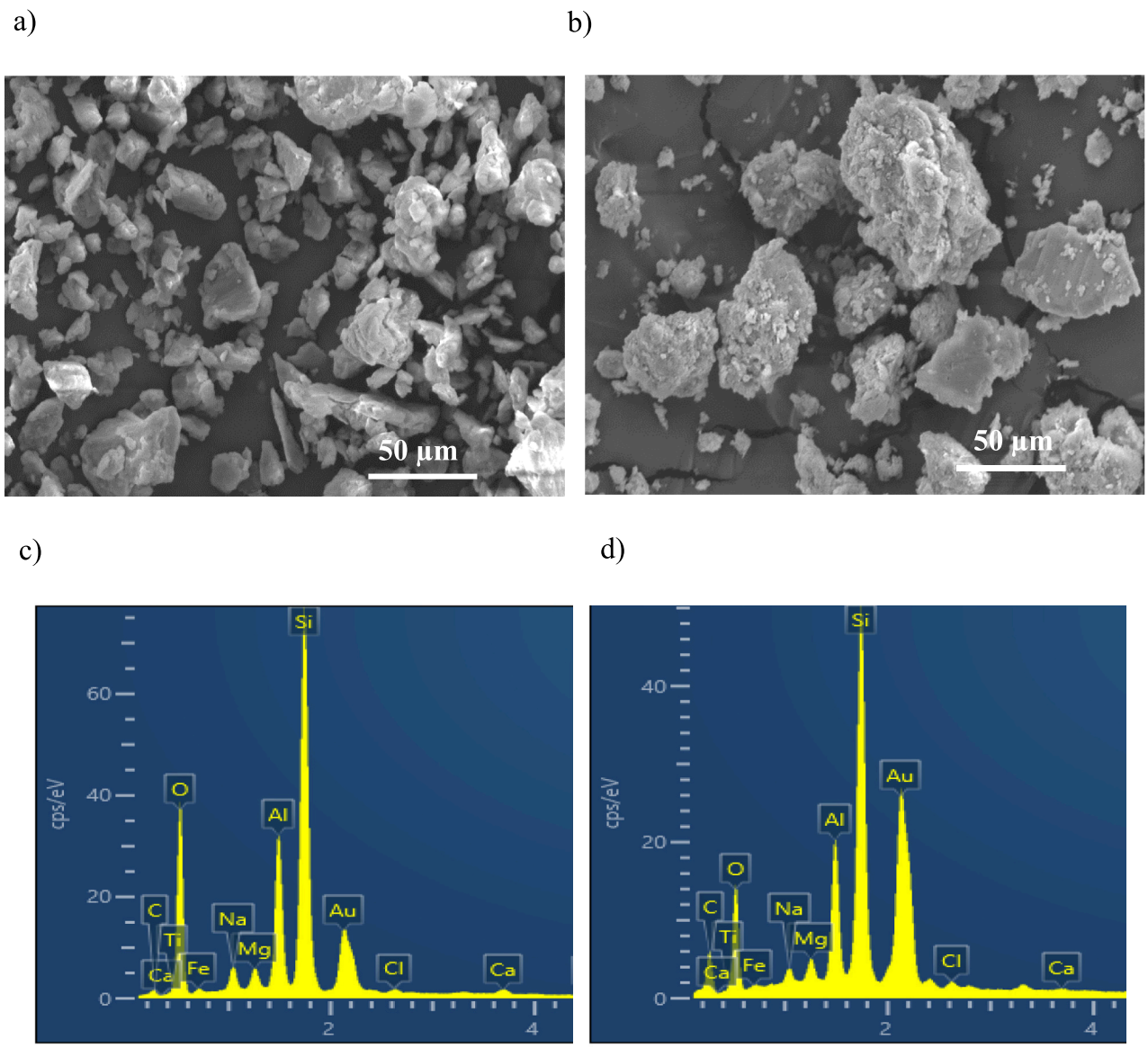

Fig. 4. SEM micrographs (1000× magnification): a) Mt. and b) MtEW4; EDS spectra from c) Mt. and d) MtEW4.

Table 5
Agar well diffusion test: diameters of inhibition zone (mm).

	MtEW2	MtEW4
A. versicolor	14 ± 1	18 ± 1
C. cladosporaides	7*	22 ± 1
C. globosum	<7	24 ± 3
E. coli	7*	10 ± 1
S. aureous	16 ± 0.3	17 ± 1.2

inhibition zones can be seen (data are expressed as mean ± SD of three experiments). In Fig. 5 photographs registers can be seen from plates at the end of the assay. The results showed that MtEW4 was active against all the strains tested while MtEW2 was active against three of them. *C. globosum* was the most resistant fungus, while *E. coli* was the most resistant bacterial strain. MtEW4 showed a clear positive antifungal activity with inhibition zones higher than 18 mm as can be corroborated in Fig. 5. Mt. was not active against all the samples. Considering that MtEW4 was the modified clay with the higher bioactivity, it was selected to integrate the formulation of the experimental waterborne paint.

Therefore, the incorporation of EO was corroborated by FTIR, XRD, TGA analysis, *ZP*, and SEM/EDS showed a higher amount of EO incorporated by MtEW4 related to MtEW2. This was evidenced by the greater range of antimicrobial activity exhibited for MtEW4 as shown in Table 5 and Fig. 5. Considering these results MtEW4 was selected to formulate the antimicrobial paints.

3.3. Characterization of paints

The viscosity of the control paints was 140 UK (PVC = 0,65) and 90 (PVC = 075) while that higher PVC was out of range. In this case, water was added before the application to obtain acceptable rheology properties. As stated before, all paints contain 5 % by weight of Mt., which due to its absorbent properties affects the viscosity of the paints, which is why the amount of Mt. that can be incorporated into the formulations is limited and, as has been seen, PVC also affects this (Tracton, 2006).

The water vapor transmission results are presented in Fig. 6. These indicate that vapor transmission depends not only on the PVC but also on the presence of MtEW4. Mainly for the control paints permeability was higher than for the paints with the Mt. hybrid at the same PVC. This difference may be attributed to the increased hydrophobicity due to organic modifier incorporation (EW/SLe) into the clay (Nagy et al.,

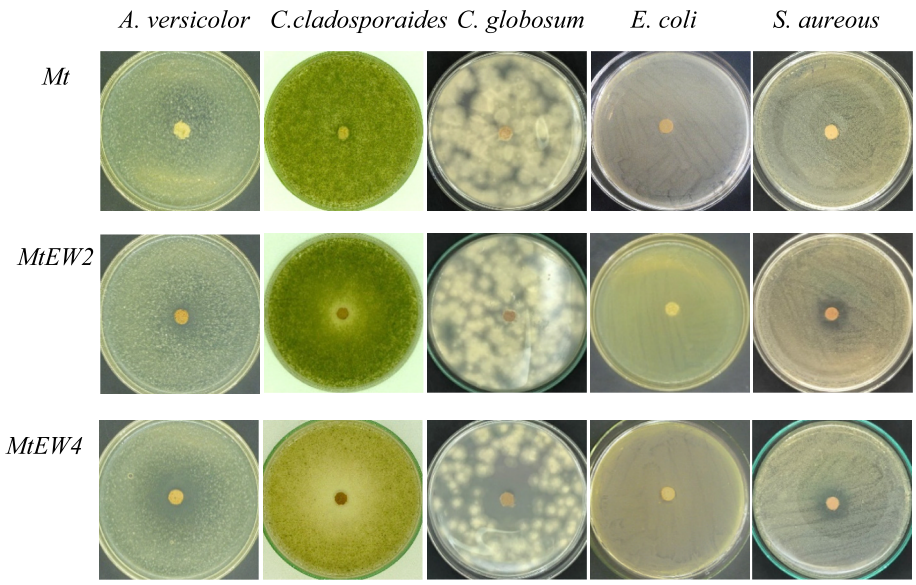

Fig. 5. Antimicrobial assay: agar well diffusion test, plates after incubation at 28 °C with Mt., MtWt2 and MtWt4.

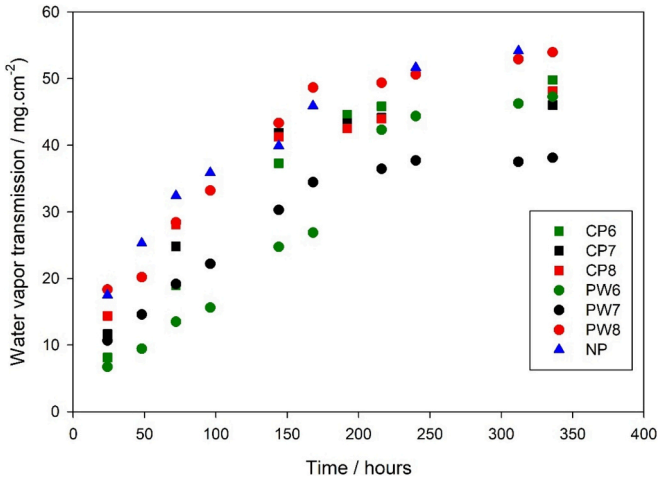

Fig. 6. Water vapor transmission of the paints (CP6, CP7, CP8, PW6, PW7, and PW8) applied to filter papers (NP refers to not painted paper).

2013).

3.4. Bacterial resistance of emulsion paint test

As shown in Fig. 7A, the control paints, CP7 and CP8, showed heavy contamination (continuous growth with indistinguishable colonies) rated (R) as 4. The same was observed with CP, while the commercial paint (SW) and the paint with PVC = 0,65 (CP6) presented a total inhibition of bacterial growth ($R = 0$). Therefore, differences in the bioresistance of the paint depending on its PVC was found. In this sense, lower PVC resulted in more resistance to bacterial growth. The paints with MWt4 were more resistant to bacterial growth with a total inhibition (R = 0) to PWt7 and PWt6 while the paint with the higher PVC (PWt8) resulted in less efficiency ($R = 4$). This is shown in Fig. 7. Therefore, PWt7 (PVC = 0,75) was efficient in preventing bacterial growth unlike what happened with the control paint without modified Mt. (CP7) with the same PVC. These results corroborate the antimicrobial activity obtained in preliminary assays with MICs ranging from 0.15 to 1.2 mg/mL that were comparable with in-can commercial biocides (e.g. CMIT and MIT) that require similar concentrations to eliminate viable *Pseudomonas aeruginosa* cells from biofilm paint tanks (do Daulisio and Schneider, 2020).

The bioactivity of the hybrid material may result from its interaction with various targets within microbial cells. The activity of EW components can primarily be attributed to their terpene, terpenoid, or phenolic constituents. Although the specific mechanisms of action for terpenoids were not fully established, several modes of action have been proposed for natural phytochemicals. These include disruption of bacterial cell membranes, modulation of efflux pump activity, inhibition of biofilm formation, and alteration in oxidative phosphorylation (Barbieri et al., 2017). Additionally, evidence suggests that both carvacrol and thymol can disrupt the outer and cytoplasmic membranes of Gram-negative bacteria, leading to their disintegration (Mahizan et al., 2019). A postulated general mechanism of antimicrobial in-can activity of the hybrid is presented in Fig. 7B.

3.5. Fungal resistance coating test

Fungal resistance test of paints (CP6, CP7, CP8, PWt6, PWt7, and PWt8) was performed by four weeks test in plates, including a commercial paint (SW). Images from the stereoscopic microscope can be seen in Fig. 8. The control paints (CP6, CP7 and CP8) inoculated with *A. versicolor, C. cladosporiodes,* and *C. globosum* presented moderate to above moderate (heavy) growth, rated (R) as 3 and 4. Unlike what happened with the *P. aeruginosa* resistance liquid paint test, no differences were observed in the performance of the control paints against the fungal strains in-film with different PVC.

SW showed total inhibition for all strains. The coatings with MtEW4 (PWt6, PWt7 and PWt8) presented moderate to heavy growth. The results showed that the tested formulations failed to prevent fungal growth efficiently. MtEW4 failed to impart its bioactivity to the coatings at the concentration used. The ineffective antifungal activity of the coatings against the studied strains may be due to the abrupt release of the EO retained in the support material or its interaction with other chemical compounds present in the system, which hinders the inhibition of ergosterol synthesis. EO can inhibit the synthesis of ergosterol, a natural component of fungal mycelial membranes essential for maintaining cellular integrity, viability, and active growth (Abdi-Moghadam et al., 2023).

In this sense, as previously highlighted, commercial biocides used to control in-film biodeterioration, such as Carbendazim, IPBC, and OIT, exhibit lower MIC values (0.5 to 10 μg/mL) than the studied EW against similar fungal strains (Adan and Samson, 2011). Furthermore,

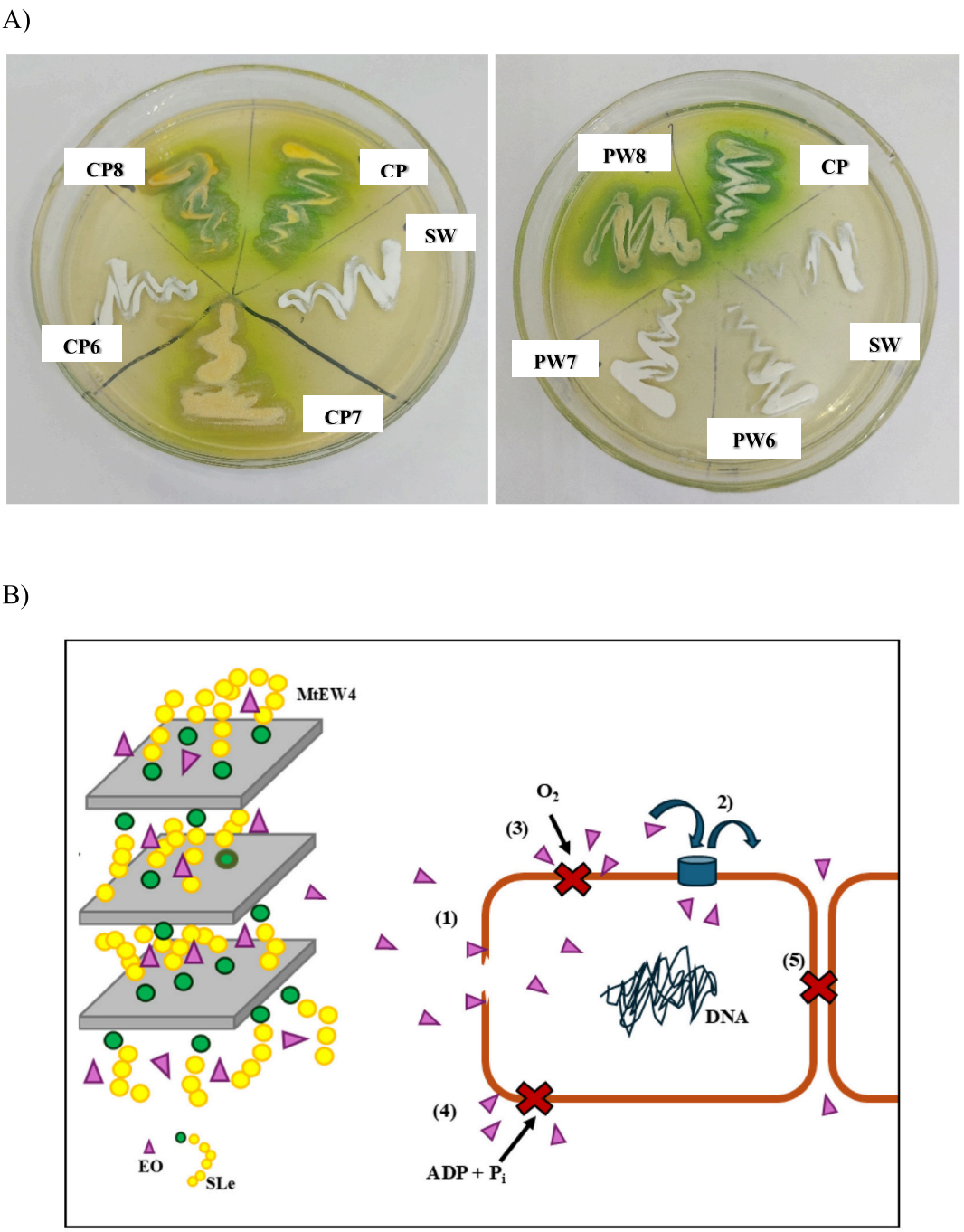

Fig. 7. A) Bacterial resistance liquid paint test against *Pseudomona aeruginosa*, plates incubated for 36 h at 30 °C with the inoculated paints (CP, CP6, CP7, CP8, PW6, PW7, PW8, and SW); B) possible antimicrobial activity mechanism of the hybrid (MtEW4): (1) disruption of the cell membrane, (2) modulation of efflux pump, (3) inhibition of oxygen uptake, (4) alteration in oxidative phosphorylation, (5) reduction of cell adherence ability and suppression of bacterial biofilm development.

isothiazolinones such as OIT are commonly employed in coating formulations at concentrations exceeding 0.5 % (5000 ppm) in most commercially available products (Romani et al., 2022). Consequently, for the effective application of the studied EW-based biocide in similar formulations, its concentration would need to exceed 0.5 %. However, the amount of modified clay in the paint cannot be increased beyond 5 % wt, as higher levels negatively affect the viscosity and applicability of the paint (Fernández et al., 2020). This presents a limitation if increasing the amount of bioactive agent in the coating is necessary. In the case of the coatings studied, and considering the hybrid (MtEW4) characterization, the organic fraction (EW/SLe) in the formulation was 1.1 %wt. Therefore, EW concentration was insufficient to inhibit fungal development. In previous research by Fernández et al. (2020), a clay hybrid with Citronellol achieved 100 % fungal inhibition in coating formulations. However, a single terpenoid was used to modify the clay in that study. In the present research, EO was employed, containing a combination of phytochemicals (e.g., terpenes, terpenoids, and phenolic compounds), leading to lower individual concentration.

Several studies support the potential of natural products in coatings. For instance, Majeed et al. (2024) demonstrated that incorporating 6 g of *Eucalyptus globulus* extract into 200 g of water-based acrylic plastic emulsion paint (3 %wt) achieved effective antimicrobial activity (Majeed et al., 2024). Similarly, Elkady et al. (2024) reported the incorporation of bioactive compounds such as 8-epi-sarcophinone and

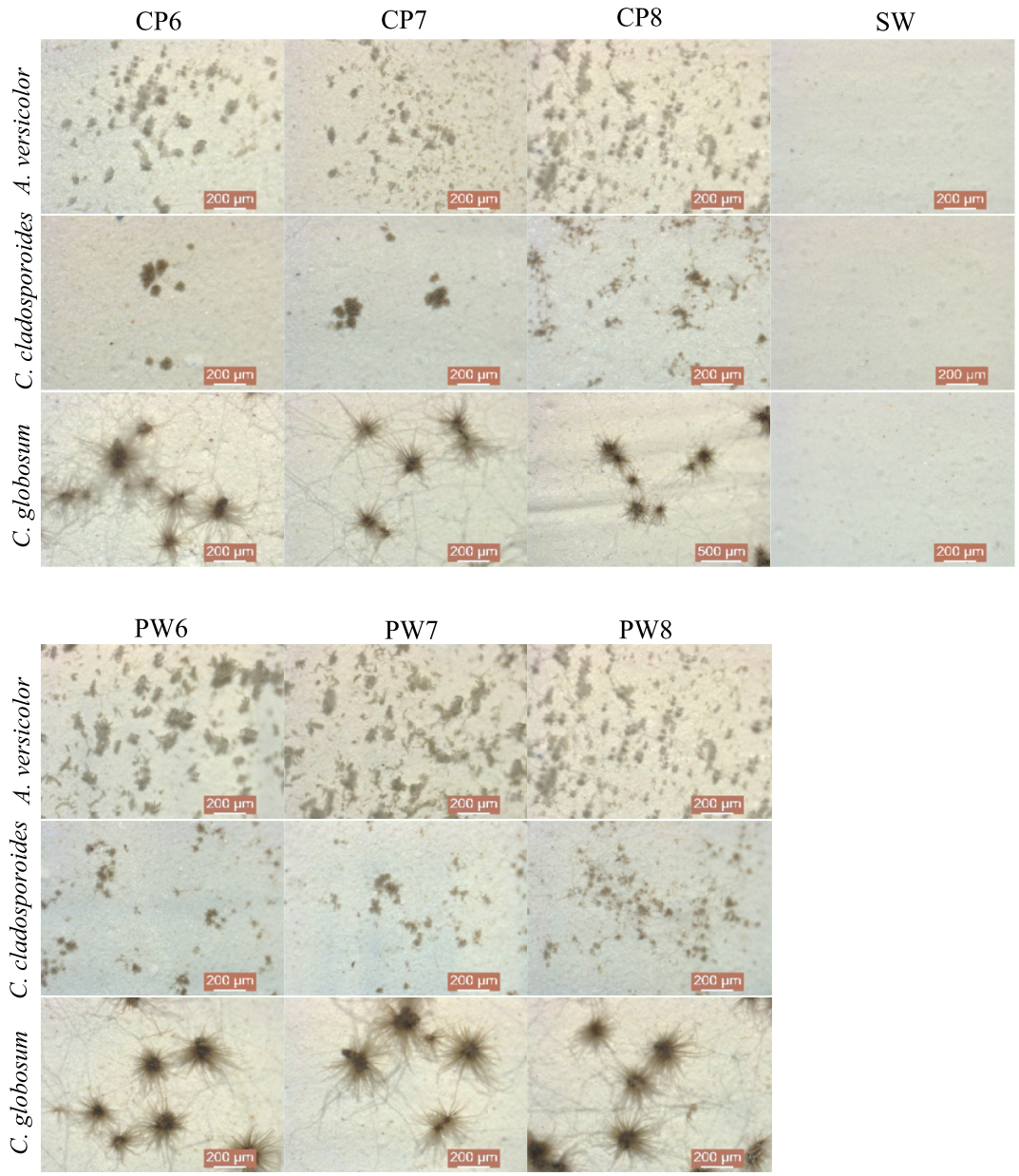

Fig. 8. Photographic register obtained from the stereoscopic microscope (80×) of fungal resistance coatings test, $t = 30$ days and $T = 28$ °C.

entsarcophine extracted from *Sarcophyton glaucum*, and Gorgosterol from *Sclerophytum leptoclados*, into paint formulations at a concentration of 0.1 %wt (Elkady et al., 2024). These coatings demonstrated superior antifouling performance (in short-time immersion trials) compared to commercial paints. In another study, Gómez de Saravia et al. (2018) incorporated eugenol, thymol, and guaiacol into exterior waterborne paint at a concentration of 2 %wt, achieving total inhibition of algae growth according to ASTM standard D5589–97 (Gómez de Saravia et al., 2018). Similarly, Gómez de Saravia et al. (2021) reported that carvacrol and isoeugenol, incorporated separately into exterior waterborne paint at a concentration of 2 %wt, exhibited total inhibition of algae growth (Gómez de Saravia et al., 2021). However, these results are from short-term trials incorporating natural products in free form. Therefore, optimizing the concentration of bioactive compounds and ensuring their stability and efficacy within complex formulations by encapsulation or using support materials remain critical to their broader application.

On the other hand, many EOs and their components were classified as GRAS for specific applications. These compounds have gained significant attention for their incorporation into functional materials, particularly in the development of antimicrobial coatings, packaging, and biomedical devices, owing to their broad-spectrum antimicrobial activity (Burt, 2004; Raut and Karuppayil, 2014). However, the large-scale application of EOs or their derivatives raises concerns about their environmental impact (Ferraz et al., 2022). The ecological risks associated with their use, particularly the introduction of residues into aquatic ecosystems and their potential effects on non-target organisms, remain insufficiently studied. Therefore, further studies are required to assess the toxicity of EOs to ensure their integration into antimicrobial materials aligns with sustainability principles, thereby reinforcing the hypothesis of their safety (Ferraz et al., 2022; Mariotti et al., 2022).

4. Conclusions

This study demonstrates the antimicrobial potential of white thyme essential oil-modified montmorillonite (MtEW4) as an innovative additive for waterborne paint formulations. The incorporation of EO into Mt. was successfully characterized through FTIR, XRD, TGA, and SEM/EDS analyses, confirming its effective retention and interaction with the clay

matrix. MtEW4 exhibited significant antimicrobial activity, particularly against bacterial strains, making it a viable alternative to conventional biocides like isothiazolinones. However, its fungal inhibition efficacy in paint formulations was limited, emphasizing the need for optimization strategies.

The antimicrobial paints with MtEW4 showed promising in-can bacterial resistance, particularly at lower PVC levels, but their fungal resistance was insufficient for in-film applications under the conditions tested. This limitation underscores the challenges of incorporating natural products like EO into complex formulations. Strategies such as increasing the concentration of bioactive agents, using single active compounds instead of mixtures, or enhancing the release control through advanced encapsulation techniques could improve their performance.

Despite these challenges, the results highlight the potential of natural biogenic compounds as environmentally friendly alternatives to commercial biocides, aligning with the growing demand for sustainable and more eco-friendly solutions in coatings. Future research should focus on addressing formulation challenges, long-term stability, and scalability to enable their practical application in protective coatings.

CRediT authorship contribution statement

Leyanet Barberia-Roque: Methodology, Investigation, Data curation. **Guillermo P. Lopez:** Methodology, Investigation, Data curation. **Erasmo Gámez-Espinosa:** Writing – original draft, Validation, Investigation. **Katerine Igal:** Supervision, Investigation. **Mariela A. Fernández:** Writing – original draft, Visualization, Validation, Investigation. **Cecilia Deyá:** Writing – original draft, Resources, Investigation. **Natalia Bellotti:** Writing – review & editing, Writing – original draft, Visualization, Supervision, Resources, Funding acquisition, Formal analysis, Data curation, Conceptualization.

Declaration of competing interest

The authors declare that they have no known competing financial interests or personal relationships that could have appeared to influence the work reported in this paper.

Acknowledgments

The authors thank to Agencia Nacional de Promoción Científica y Tecnológica (ANCyT), Consejo Nacional de Investigaciones Científicas y Técnicas (CONICET), Comisión de Investigaciones Científicas de la Provincia de Buenos Aires (CICPBA) and Universidad Nacional de La Plata (UNLP) for their support. They also thank to: the service sector of the CIDEPINT (Ing. Mateo Paez, Diego Tunessi, and Ing. María José Ayala), Claudio Cerruti for the FTIR spectra, the technical support of the Ing. Pablo Bellotti, and the SeMFI (Servicio de Microscopía y Microanálisis-LIMF/Facultad de Ingeniería de la UNLP). They thank to Diransa for providing the resin and additives.

Data availability

Data will be made available on request.

References

Abdi-Moghadam, Z., Mazaheri, Y., Rezagholizade-shirvan, A., Mahmoudzadeh, M., Sarafraz, M., Mohtashami, M., Shokri, S., Ghasemi, A., Nickfar, F., Darroudi, M., Hossieni, H., Hadian, Z., Shamloo, E., Rezaei, Z., 2023. The significance of essential oils and their antifungal properties in the food industry: a systematic review. Heliyon 9, e21386. https://doi.org/10.1016/j.heliyon.2023.e21386.

Adan and Samson, 2011. Fundamentals of mold growth in indoor environments and strategies for healthy living. In: Fundamentals of Mold Growth in Indoor Environments and Strategies for Healthy Living. https://doi.org/10.3920/978-90-8686-722-6.

Ameziane, N., Boubaker, H., Boudyach, H., Msanda, F., Jilal, A., Benaoumar, A.A., 2007. Original article antifungal activity of Moroccan plants against citrus fruit pathogens. J. Agron. 27, 273–277.

Andrade, M.A., Ribeiro-Santos, R., Costa Bonito, M.C., Saraiva, M., Sanches-Silva, A., 2018. Characterization of rosemary and thyme extracts for incorporation into a whey protein based film. Lwt 92, 497–508. https://doi.org/10.1016/j.lwt.2018.02.041.

ASTM, D. 5590, 2001. Standard test method for determining the resistance of paint films and related coatings to fungal defacement by accelerated four-week. In: Stand. Test Method Determ. Resist. Paint Film. Relat. Coatings to Fungal Defacement by Accel. Four-Week, i, pp. 10–13. https://doi.org/10.1520/D5590-17R21.2.

ASTM D2574-16, 2020. Standard test method for resistance of emulsion paints in the container to attack by microorganisms. Biodegradation 1–4.

Barbieri, R., Coppo, E., Marchese, A., Daglia, M., Sobarzo-Sánchez, E., Nabavi, S.F., Nabavi, S.M., 2017. Phytochemicals for human disease: an update on plant-derived compounds antibacterial activity. Microbiol. Res. 196, 44–68. https://doi.org/10.1016/j.micres.2016.12.003.

Barraqué, F., Montes, M.L., Fernández, M.A., Mercader, R.C., Candal, R.J., Torres Sánchez, R.M., 2018. Synthesis and characterization of magnetic-montmorillonite and magnetic-organo-montmorillonite: surface sites involved on cobalt sorption. J. Magn. Magn. Mater. 466, 376–384. https://doi.org/10.1016/j.jmmm.2018.07.052.

Bellotti, N., Deyá, C., 2020. Waterborne functional paints to control biodeterioration. In: Handb. Waterborne Coatings, pp. 155–179. https://doi.org/10.1016/b978-0-12-814201-1.00007-x.

Bellotti, N., Romagnoli, R., Quintero, C., Domínguez-Wong, C., Ruiz, F., Deyá, C., 2015. Nanoparticles as antifungal additives for indoor water borne paints. Prog. Org. Coat. 86, 33–40. https://doi.org/10.1016/j.porgcoat.2015.03.006.

Bergaya, F., Lagaly, G., 2013. Purification of natural clays. In: Developments in Clay Science, 2nd ed. Elsevier Ltd. https://doi.org/10.1016/B978-0-08-098258-8.00008-0.

Bonilla, J., Sobral, P.J.A., 2016. Investigation of the physicochemical, antimicrobial and antioxidant properties of gelatin-chitosan edible film mixed with plant ethanolic extracts. Food Biosci. 16, 17–25. https://doi.org/10.1016/j.fbio.2016.07.003.

Burt, S., 2004. Essential oils: their antibacterial properties and potential applications in foods - a review. Int. J. Food Microbiol. 94, 223–253. https://doi.org/10.1016/j.ijfoodmicro.2004.03.022.

Cámara, M., Green, W., MacPhee, C.E., Rakowska, P.D., Raval, R., Richardson, M.C., Slater-Jefferies, J., Steventon, K., Webb, J.S., 2022. Economic significance of biofilms: a multidisciplinary and cross-sectoral challenge. NPJ Biofilms Microbiomes 8, 1–8. https://doi.org/10.1038/s41522-022-00306-y.

Câmara, J.S., Perestrelo, R., Ferreira, R., Berenguer, C.V., Pereira, J.A.M., Castilho, P.C., 2024. Plant-derived terpenoids: a plethora of bioactive compounds with several health functions and industrial applications—a comprehensive overview. Molecules 29. https://doi.org/10.3390/molecules29163861.

Capelezzo, A.P., Celuppi, L.C.M., Macuvele, D.L.P., Zeferino, R.C.F., Zanetti, M., Bender, J.P., de Mello, J.M.M., Fiori, M.A., Riella, H.G., 2023. Obtaining and characterization of bentonite organophilic incorporated with geranyl acetate and its application as mycotoxins' binder in simulated gastrointestinal fluids. Appl. Clay Sci. 237. https://doi.org/10.1016/j.clay.2023.106915.

Chen, W., Viljoen, A.M., 2022. Geraniol – a review update. S. Afr. J. Bot. 150, 1205–1219. https://doi.org/10.1016/j.sajb.2022.09.012.

Chen, B., Jia, Y., Zhang, M., Li, X., Yang, J., Zhang, X., 2019. Facile modification of sepiolite and its application in superhydrophobic coatings. Appl. Clay Sci. 174, 1–9. https://doi.org/10.1016/j.clay.2019.03.016.

Chen, Y. Qing, Wang, S. Qing, Tong, X.Y., Kang, X., 2022a. Crystal transformation and self-assembly theory of microbially induced calcium carbonate precipitation. Appl. Microbiol. Biotechnol. 106, 3555–3569. https://doi.org/10.1007/s00253-022-11938-7.

Chen, Y., Wang, S., Tong, X.Y., Kang, X., 2022b. Towards the sustainable fine control of microbially induced calcium carbonate precipitation. J. Clean. Prod. 377, 134395. https://doi.org/10.1016/j.jclepro.2022.134395.

Ciğeroğlu, Z., El Messaoudi, N., Şenol, Z.M., Başkan, G., Georgin, J., Gubernat, S., 2024. Clay-based nanomaterials and their adsorptive removal efficiency for dyes and antibiotics: a review. Mater. Today Sustain. 26. https://doi.org/10.1016/j.mtsust.2024.100735.

CLSI, Dolinsky, A.L., Ohiro, R.K., Fan, W., Xiao, C., Wu, F., National Committee for Clinical Laboratory Standards, 2019. Performance standard for antimicrobial susceptibility testing. Document M100–S10. J. Int. Med. Res. 46, 18.

Czímerová, A., Bujdák, J., Dohrmann, R., 2006. Traditional and novel methods for estimating the layer charge of smectites. Appl. Clay Sci. 34, 2–13. https://doi.org/10.1016/j.clay.2006.02.008.

de Oliveira, L.H., Trigueiro, P., Souza, J.S.N., de Carvalho, M.S., Osajima, J.A., da Silva-Filho, E.C., Fonseca, M.G., 2022. Montmorillonite with essential oils as antimicrobial agents, packaging, repellents, and insecticides: an overview. Colloids Surf. B: Biointerfaces 209. https://doi.org/10.1016/j.colsurfb.2021.112186.

do Daulisio, M.C.Z., Schneider, R.P., 2020. Inactivation of *Pseudomonas aeruginosa* MDC by isothiazolones and biocide stabilizing agents. Int. Biodeterior. Biodegrad. 155. https://doi.org/10.1016/j.ibiod.2020.105090.

Eftekhari, A., Khusro, A., Ahmadian, E., Dizaj, S.M., Dinparast, L., Bahadori, M.B., Hasanzadeh, A., Cucchiarini, M., 2021. Phytochemical and nutra-pharmaceutical attributes of Mentha spp.: a comprehensive review. Arab. J. Chem. 14, 103106. https://doi.org/10.1016/j.arabjc.2021.103106.

Elkady, E.M., Tadros, H.R.Z., Soliman, Y.A., Raafat, M., Abdel-Tawab, A.M., 2024. Marine antifouling agents based on bioactive compounds isolated from Red Sea soft

corals Sarcophyton glaucum and Sclerophytum leptoclados. Egypt. J. Aquat. Res. 50, 234–240. https://doi.org/10.1016/j.ejar.2024.06.004.
Farina Farizan, A., Nurhanis Amira Nik Mohd Sukrri, N., Mohd Ramzi, M., Najihah Rawi, N., Izzati Abd Rahman, N., Bakar, K., Yong Fu Siong, J., Sifzizul Tengku Muhammad, T., Khusairi Azemi, A., Ismail, N., 2024. *Melaleuca cajuputi*: metabolites profiling and its potential against biofouling. Egypt. J. Aquat. Res. 50, 342–347. https://doi.org/10.1016/j.ejar.2024.06.005.
Fattahi, R., Kalalagh, K.F., Bahrami, A., 2023. Correlating the pre–emulsion conditions of film–making with the characteristics of active chitosan films containing orange essential oil (*Citrus sinensis* L.). Prog. Org. Coat. 174. https://doi.org/10.1016/j.porgcoat.2022.107270.
Felgueiras, F., Mourão, Z., de Oliveira Fernandes, E., Gabriel, M.F., 2022. Airborne bacterial and fungal concentrations and fungal diversity in bedrooms of infant twins under 1 year of age living in Porto. Environ. Res. 206. https://doi.org/10.1016/j.envres.2021.112568.
Fernández Solarte, A.M., Villarroel-Rocha, J., Morantes, C.F., Montes, M.L., Sapag, K., Curutchet, G., Torres Sánchez, R.M., 2019. Insight into surface and structural changes of montmorillonite and organomontmorillonites loaded with Ag. C. R. Chim. 22, 142–153. https://doi.org/10.1016/j.crci.2018.09.006.
Fernández, M.A., Barberia Roque, L., Gámez Espinosa, E., Deyá, C., Bellotti, N., 2020. Organo-montmorillonite with biogenic compounds to be applied in antifungal coatings. Appl. Clay Sci. 184, 105369. https://doi.org/10.1016/j.clay.2019.105369.
Ferraz, C.A., Pastorinho, M.R., Palmeira-de-Oliveira, A., Sousa, A.C.A., 2022. Ecotoxicity of plant extracts and essential oils: a review. Environ. Pollut. 292, 118319. https://doi.org/10.1016/j.envpol.2021.118319.
Freitas, E.D., Bataglioli, R.A., Oshodi, J., Beppu, M.M., 2022. Antimicrobial peptides and their potential application in antiviral coating agents. Colloids Surf. B: Biointerfaces 217. https://doi.org/10.1016/j.colsurfb.2022.112693.
Gamba, M., Flores, F.M., Madejová, J., Sánchez, R.M.T., 2015. Comparison of imazalil removal onto montmorillonite and nanomontmorillonite and adsorption surface sites involved: an approach for agricultural wastewater treatment. Ind. Eng. Chem. Res. 54, 1529–1538. https://doi.org/10.1021/ie5035804.
Gámez-Espinosa, E., Barberia-Roque, L., Obidi, O.F., Deyá, C., Bellotti, N., 2020a. Antifungal applications for nano-additives synthesized with a bio-based approach. Adv. Nat. Sci. Nanosci. Nanotechnol. 11, 015019. https://doi.org/10.1088/2043-6254/ab790f.
Gámez-Espinosa, E., Bellotti, N., Deyá, C., Cabello, M., 2020b. Mycological studies as a tool to improve the control of building materials biodeterioration. J. Build. Eng. 32, 101738. https://doi.org/10.1016/j.jobe.2020.101738.
Gámez-Espinosa, E., Deyá, C., Ruiz, F., Bellotti, N., 2022. LONG-TERM field study of a Waterborne paint with a nano-additive for biodeterioration control. J. Build. Eng. 50. https://doi.org/10.1016/j.jobe.2022.104148.
García-Guzmán, P., Medina-Torres, L., Josefa Bernad-Bernad, M., Calderas, F., Manero, O., 2023. Study of the cholesterol adsorption and characterization of montmorillonite and bentonite clay. Mater. Today Commun. 35. https://doi.org/10.1016/j.mtcomm.2023.105604.
Giannakas, A., Tsagkalias, I., Achilias, D.S., Ladavos, A., 2017. A novel method for the preparation of inorganic and organo-modified montmorillonite essential oil hybrids. Appl. Clay Sci. 146, 362–370. https://doi.org/10.1016/j.clay.2017.06.018.
Gillatt, J., Julian, K., Brett, K., Goldbach, M., Grohmann, J., Heer, B., Nichols, K., Roden, K., Rook, T., Schubert, T., Stephan, I., 2015. The microbial resistance of polymer dispersions and the efficacy of polymer dispersion biocides - a statistically validated method. Int. Biodeterior. Biodegrad. 104, 32–37. https://doi.org/10.1016/j.ibiod.2015.04.028.
Gómez de Saravia, S.G., Rastelli, S.E., Blustein, G., Viera, M.R., 2018. Natural compounds as potential algaecides for waterborne paints. J. Coat. Technol. Res. 15, 1191–1200. https://doi.org/10.1007/s11998-018-0099-7.
Gómez de Saravia, S.G., Rastelli, S.E., Blustein, G., Viera, M.R., 2021. Antibacterial and algaecide activity of three natural compounds: lab-test approaches on their potential use in paint formulations. J. Build. Eng. 43. https://doi.org/10.1016/j.jobe.2021.102560.
Gonçalves, N.D., de Pena, F.L., Sartoratto, A., Derlamelina, C., Duarte, M.C.T., Antunes, A.E.C., Prata, A.S., 2017. Encapsulated thyme (*Thymus vulgaris*) essential oil used as a natural preservative in bakery product. Food Res. Int. 96, 154–160. https://doi.org/10.1016/j.foodres.2017.03.006.
Guimarães, A.C., Meireles, L.M., Lemos, M.F., Guimarães, M.C.C., Endringer, D.C., Fronza, M., Scherer, R., 2019. Antibacterial activity of terpenes and terpenoids present in essential oils. Molecules 24, 1–12. https://doi.org/10.3390/molecules24132471.
He, H., Frost, R.L., Bostrom, T., Yuan, P., Duong, L., Yang, D., Xi, Y., Kloprogge, J.T., 2006. Changes in the morphology of organoclays with HDTMA+ surfactant loading. Appl. Clay Sci. 31, 262–271. https://doi.org/10.1016/j.clay.2005.10.011.
He, Q., Zhu, R., Chen, Q., Zhu, Y., Yang, Y., Du, J., Zhu, J., He, H., 2020. One-pot synthesis of the reduced-charge montmorillonite via molten salts treatment. Appl. Clay Sci. 186, 105429. https://doi.org/10.1016/j.clay.2019.105429.
Hendessi, S., Sevinis, E.B., Unal, S., Cebeci, F.C., Menceloglu, Y.Z., Unal, H., 2016. Antibacterial sustained-release coatings from halloysite nanotubes/waterborne polyurethanes. Prog. Org. Coat. 101, 253–261. https://doi.org/10.1016/j.porgcoat.2016.09.005.
Hossain, S.I., Kukushkina, E.A., Izzi, M., Sportelli, M.C., Picca, R.A., Ditaranto, N., Cioffi, N., 2023. A review on montmorillonite-based nanoantimicrobials: state of the art. Nanomaterials 13, 1–34. https://doi.org/10.3390/nano13050848.
Kakakhel, M.A., Wu, F., Gu, J.D., Feng, H., Shah, K., Wang, W., 2019. Controlling biodeterioration of cultural heritage objects with biocides: a review. Int. Biodeterior. Biodegrad. 143, 104721. https://doi.org/10.1016/j.ibiod.2019.104721.
Lagaly, G., Ogawa, M., Dékány, I., 2006. Chapter 7.3 Clay Mineral Organic Interactions. Dev. Clay Sci. 1, 309–377. https://doi.org/10.1016/S1572-4352(05)01010-X.
Lagrouh, F., Dakka, N., Bakri, Y., 2017. The antifungal activity of Moroccan plants and the mechanism of action of secondary metabolites from plants. J. Mycol. Médicale 27, 303–311. https://doi.org/10.1016/j.mycmed.2017.04.008.
Lindholm, J., Boily, J.F., Holmboe, M., 2019. Deconvolution of smectite hydration isotherms. ACS Earth Space Chem. 3, 2490–2498. https://doi.org/10.1021/acsearthspacechem.9b00178.
Liu, W., Zhuang, L., Liu, J., Liu, Y., Wang, L., He, Y., Yang, G., Shen, F., Zhang, X., Zhang, Y., 2021. Make the building walls always clean: a durable and anti-bioadhesive diatomaceous earth@SiO2 coating. Constr. Build. Mater. 301, 124293. https://doi.org/10.1016/j.conbuildmat.2021.124293.
Madejová, J., 2003. FTIR techniques in clay mineral studies. Vib. Spectrosc. 31, 1–10. https://doi.org/10.1016/S0924-2031(02)00065-6.
Magnoli, A.P., Tallone, L., Rosa, C.A.R., Dalcero, A.M., Chiacchiera, S.M., Torres Sanchez, R.M., 2008. Commercial bentonites as detoxifier of broiler feed contaminated with aflatoxin. Appl. Clay Sci. 40, 63–71. https://doi.org/10.1016/j.clay.2007.07.007.
Mahizan, N.A., Yang, S., Moo, C.-L., Song, A.A.-L., 2019. Terpene derivatives as a potential agent against. Molecules 24, 1–21.
Majeed, H., Iftikhar, T., Ashir Nadeem, M., Altaf Nazir, M., 2024. Green synthesis of *Eucalyptus globulus* zinc nanoparticles and its use in antimicrobial insect repellent paint formulation in bulk industrial production. Heliyon 10, e24467. https://doi.org/10.1016/j.heliyon.2024.e24467.
Majhi, S., Arora, A., Mishra, A., 2019. Surface immobilization of a short antimicrobial peptide (AMP) as an antibacterial coating. Materialia 6, 100350. https://doi.org/10.1016/j.mtla.2019.100350.
Mamusa, M., Resta, C., Sofroniou, C., Baglioni, P., 2021. Encapsulation of volatile compounds in liquid media: fragrances, flavors, and essential oils in commercial formulations. Adv. Colloid Interf. Sci. 298, 102544. https://doi.org/10.1016/j.cis.2021.102544.
Mangalagiri, N.P., Panditi, S.K., Jeevigunta, N.L.L., 2021. Antimicrobial activity of essential plant oils and their major components. Heliyon 7, e06835. https://doi.org/10.1016/j.heliyon.2021.e06835.
Marco, A., Santos, S., Caetano, J., Pintado, M., Vieira, E., Moreira, P.R., 2020. Basil essential oil as an alternative to commercial biocides against fungi associated with black stains in mural painting. Build. Environ. 167, 106459. https://doi.org/10.1016/j.buildenv.2019.106459.
Mardones, L.E., Legnoverde, M.S., Monzón, J.D., Bellotti, N., Basaldella, E.I., 2019. Increasing the effectiveness of a liquid biocide component used in antifungal waterborne paints by its encapsulation in mesoporous silicas. Prog. Org. Coat. 134. https://doi.org/10.1016/j.porgcoat.2019.04.058.
Mariotti, M., Lombardini, G., Rizzo, S., Scarafile, D., Modesto, M., Truzzi, E., Benvenuti, S., Elmi, A., Bertocchi, M., Fiorentini, L., Gambi, L., Scozzoli, M., Mattarelli, P., 2022. Potential applications of essential oils for environmental sanitization and antimicrobial treatment of intensive livestock infections. Microorganisms 10, 1–21. https://doi.org/10.3390/microorganisms10040822.
Mendonça, F.G., Filho, E.J.S., Bertoli, A.C., Fernández, M.A., Torres Sánchez, R.M., Lago, R.M., 2019. Use of montmorillonite to recover carboxylic acids from aqueous medium. Sep. Purif. Technol. 229, 115751. https://doi.org/10.1016/j.seppur.2019.115751.
Nagy, K., Bíró, G., Berkesi, O., Benczédi, D., Ouali, L., Dékány, I., 2013. Intercalation of lecithins for preparation of layered nanohybrid materials and adsorption of limonene. Appl. Clay Sci. 72, 155–162. https://doi.org/10.1016/j.clay.2012.11.008.
Nakhli, A., Mbouga, M.G.N., Bergaoui, M., Khalfaoui, M., Cretin, M., Huguet, P., 2018. Modeling of essential oils adsorption onto clays towards a better understanding of their interactions. J. Mol. Liq. 249, 132–143. https://doi.org/10.1016/j.molliq.2017.11.012.
Qiu, Q., Gu, Y., Ren, Y., Ding, H., Hu, C., Wu, D., Mou, J., Wu, Z., Dai, D., 2024. Research progress on eco-friendly natural antifouling agents and their antifouling mechanisms. Chem. Eng. J. 495, 153638. https://doi.org/10.1016/j.cej.2024.153638.
Raut, J.S., Karuppayil, S.M., 2014. A status review on the medicinal properties of essential oils. Ind. Crop. Prod. 62, 250–264. https://doi.org/10.1016/j.indcrop.2014.05.055.
Romani, M., Warscheid, T., Nicole, L., Marcon, L., Di Martino, P., Suzuki, M.T., Lebaron, P., Lami, R., 2022. Current and future chemical treatments to fight biodeterioration of outdoor building materials and associated biofilms: moving away from ecotoxic and towards efficient, sustainable solutions. Sci. Total Environ. 802, 149846. https://doi.org/10.1016/j.scitotenv.2021.149846.
Ryu, V., McClements, D.J., Corradini, M.G., McLandsborough, L., 2018. Effect of ripening inhibitor type on formation, stability, and antimicrobial activity of thyme oil nanoemulsion. Food Chem. 245, 104–111. https://doi.org/10.1016/j.foodchem.2017.10.084.
Sánchez Espinosa, K.C., Rodríguez Davydenko, S., Rojas Flores, T.I., Fernández-González, M., Almaguer, M., 2024. Xerophilic and cellulolytic fungi in the indoor air of houses in Havana. Int. Biodeterior. Biodegrad. 188. https://doi.org/10.1016/j.ibiod.2024.105730.
Stupar, M., Grbić, M.L., Džamić, A., Unković, N., Ristić, M., Jelikić, A., Vukojević, J., 2014. Antifungal activity of selected essential oils and biocide benzalkonium chloride against the fungi isolated from cultural heritage objects. S. Afr. J. Bot. 93, 118–124. https://doi.org/10.1016/j.sajb.2014.03.016.
Tracton, A.A., 2006. Coatings Technology Handbook, Third edition. Taylor & Francis Group.
U.S. Food and Drug Administration-FDA, Food and Drug Administration, Department of Health and Human Services, 2024. Part 172 – food additives permitted for direct

addition to food for human consumption. Subpart F – flavoring agents and related substances, 515 – synthetic flavoring substances and adj. In: Code of Federal Regulations, 21 CFR 172.515. Title 21 – Food and Drugs, vol. 3. Silver spring.

Walentowska, J., Foksowicz-Flaczyk, J., 2013. Thyme essential oil for antimicrobial protection of natural textiles. Int. Biodeterior. Biodegrad. 84, 407–411. https://doi.org/10.1016/j.ibiod.2012.06.028.

Wang, X., Zhu, C., Hu, Y., Zhang, Z., Zhang, B., 2023. Development and application of cinnamaldehyde-loaded halloysite nanotubes for the conservation of stone cultural heritage. Appl. Clay Sci. 236, 106886. https://doi.org/10.1016/j.clay.2023.106886.

Weber, D.J., Kanamori, H., Rutala, W.A., 2016. "No touch" technologies for environmental decontamination: focus on ultraviolet devices and hydrogen peroxide systems. Curr. Opin. Infect. Dis. 29, 424–431. https://doi.org/10.1097/QCO.0000000000000284.

Xiao, H., Liang, G., Komarneni, S., Chen, Y., Qiu, J., Ma, S., Zhu, J., Wang, G., 2024. A novel and efficient method for synthesizing reduced charge montmorillonite. Surf. Interfaces 53, 105033. https://doi.org/10.1016/j.surfin.2024.105033.

Zhou, W., Liu, T., Zhang, Z., Wang, G., Zhang, S., Wei, H., Wang, Q., Ma, T., Li, R., 2023. Synthesis and evaluation of phenolic capsaicin-derived self-polymers for antibacterial activity. Process Biochem. 132, 30–40. https://doi.org/10.1016/j.procbio.2023.07.006.

Zhuang, K., Tang, H., Guo, H., Yuan, S., 2023. Geraniol prevents helicobacterium pylori-induced human gastric cancer signalling by enhancing peroxiredoxin-1 expression in GES-1 cells. Microb. Pathog. 174, 105937. https://doi.org/10.1016/j.micpath.2022.105937.